THERMO-ECONOMIC EVALUATION OF ORCS FOR VARIOUS WORKING FLUIDS

Pardeep Garg[1*], Matthew S. Orosz[2], Pramod Kumar[1+], Pradip Dutta[1#]

[1]Indian Institute of Science Bangalore
C V Raman Ave, Bengaluru, Karnataka, India
[*]E-mail: pardeep_1127@yahoo.com
[+]E-mail: pramod_k24@yahoo.com
[#]E-mail: pradip@mecheng.iisc.ernet.in

[2]Massachusetts Institute of Technology
Cambridge, MA, USA
E-mail: mso@mit.edu

ABSTRACT

A general thermoeconomic optimization of sub 500kW$_e$ ORCs is developed using a 7-dimensional design space, with minimum investment cost per unit of nameplate electricity production as an objective function. Parameters used include working fluid, heat source temperature, pinch in condenser, boiler (HEX) and regenerator, expander inlet pressure and air cooled condenser area. Optimized power block configurations are presented for the application of ORCs with geothermal or waste heat sources and solar heat input for power scales of 5, 50 and 500 kWe to facilitate rapid selection of design parameters across a range of thermal regimes. While R152a yields the lowest cost ORCs in the case of the former, isopentane is found to be more cost effective in the latter case for heat source temperatures between 125 and 275 ºC.

1. INTRODUCTION

Increasing electricity demand necessitates the utilization of diverse energy resources, including the exergy potential of low temperature (< 300 °C) heat streams such as geothermal, waste heat from industrial processes or low concentration factor (< 100) solar collector systems. At sub steam-Rankine temperatures, the organic Rankine cycle (ORC) is a scalable thermodynamic solution for converting thermal resources (Velez et al., 2012) that can be configured to meet variable project demands. These resources are widely distributed in space, and consequently investment decisions for such inherently distributed generation projects require costly site and application-specific engineering and economic analysis. The design of ORC equipment optimized for unique resources and applications also involves a number of trade-offs and adds cost to projects.

Various working fluids have been proposed in the literature with optimized selections based on thermodynamic performance (Hung et al. 2010, Maizza and Maizza 2001, Wei et al., 2007 and Wang et al., 2011). However, when the strategic objective is minimized investment cost for a specific level of power output, the corresponding configuration and design operating conditions need not occur at the point of maximum efficiency (Quoilin et al. 2011). Work by Tempesti and Fiaschi (2013) and Lecompte et al. (2013) supports the above observation and underscores the need for a detailed thermo-economic evaluation of various ORC design parameters for comparison on an equivalent basis and generalizable across a wide range of ORC applications. This work presents such a study wherein the key design parameters influencing the specific cost of power from an air-cooled ORC are identified and used to formulate a 7-dimensional space to search for the minimum costs for applications with a) geothermal or waste heat sources and b) solar ORCs. Corresponding maps of operating parameters are generated to facilitate ORC engineers in the design of economic systems within constraints such as available heat source temperatures, maximum expander inlet pressures imposed, etc. Further, the effect of power scaling on these specific costs is evaluated for ORC capacities between 5 and 500kW$_e$.

2. Cycle details

The physical system considered in this paper consists of an ORC energized by a heat transfer fluid (HTF) that could be heated in two ways, forming Case A and B as follows:

Case A: The HTF gains enthalpy from geothermal or industrial waste heat or similarly relatively inexpensive sources (Figure 1). Here, the minimization of costs for a specific power output (i.e. $/kW) are driven by the ORC capital expenditure at its performance envelope.

Case B: An ORC is coupled to a thermo-solar collector field via a thermal storage system (Figure 2) that maintains steady output in the ORC throughout the day. Here, the thermal source is a parabolic trough collector with significant cost. The optimization strategy in this case would be to configure the ORC to minimize the total system cost for a specific power output.

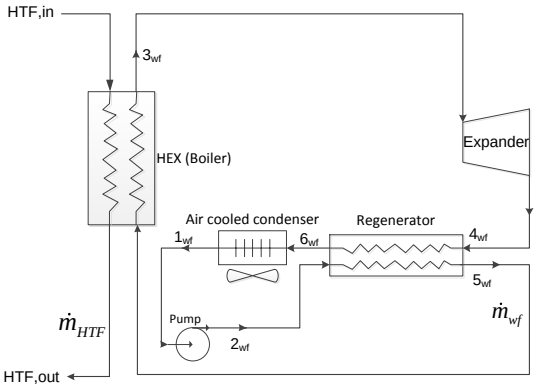

Figure 1. Schematic of an ORC which can be connected to a geothermal or waste heat recovery source.

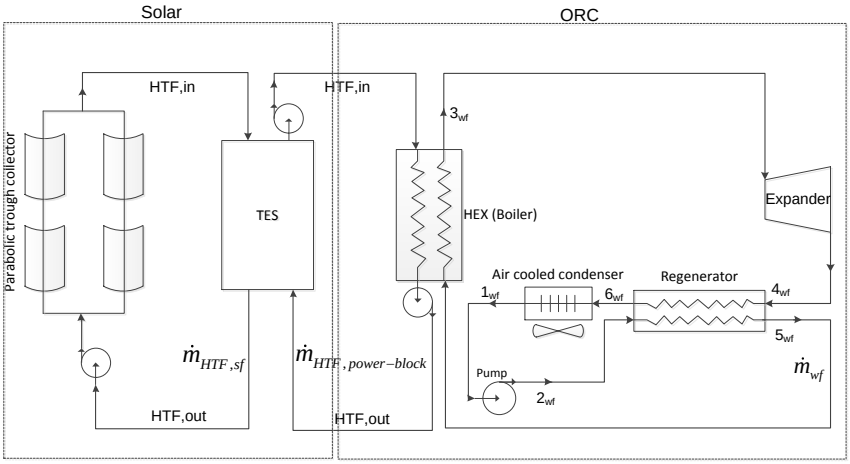

Figure 2. Schematic of an ORC connected to a solar source.

ORC component details:

The major components in a typical ORC include expander, heat exchangers (boiler, regenerator), air-cooled condenser (ACC), pumps, and VFD drives. For sub MWe ORC, positive displacement expanders are appropriate at the smaller scales where turbo-expanders suffer from high rotational speeds and lower isentropic efficiencies (Fiaschi *et al.*, 2012).

For the working fluid pump, a plunger type positive displacement device suitable for sub-MWe ORCs is coupled to a variable frequency drive to achieve the designed mass flow rates. The regenerator and boiler are modeled as plate heat exchangers which are limited to 60 bar and hence the high side cycle pressure ($p_{3,wf}$) is restricted to 60 bar. These heat exchangers are modeled for a pressure drop of 1.5 % of their pressures at the inlets on both cold and hot side along the length of heat exchanger using heat transfer and pressure drop correlations from literature sources (Martin, 1996 for single phase heat transfer, Würfel et al., 2004 for two phase heat transfer and Pioro et al., 2004 for heat transfer in

supercritical regime) for sub- as well as trans-critical cycles. A 1-D numerical approach is employed to model these exchangers, accounting for the variation in the thermo-physical properties of the working fluid during heat transfer. The temperature profile of the HTF in the boiler is determined by a procedure based on minimization of entropy generation in the boiler (Garg et al., 2013). The expander chosen is scroll (connected to an electric generator) for which the overall isentropic efficiency is assumed to be 65% from thermal to electrical (Lemort et al., 2009). The cost function for scroll expanders is generated using a database of existing scroll compressors for HVAC applications. In the case of volume ratio > 2.89, two or more scrolls are used in series. The condenser is air cooled and designed in such a way that the overall system cost is optimized taking into account its fan power. Commercially available condenser unit sizes are used in the analysis with the smallest and the largest surficial area ranging from 0.5 m^2 to 9.2 m^2. In case of higher power levels requiring larger surficial areas (>9.2 m^2), parallel units of condenser are considered. Modeling details of the condenser can be found in the Masters thesis of Monifa Fela Wright (2000). Major instruments considered in the power block include temperature and pressure sensors, flow meter, current transducers, data acquisition system, data processing and control systems. Details of the cost functions used in the analysis can be found in appendix A. Costs pertaining to the pipes and other accessories are not considered in this paper.

Solar-ORC details:

In the solar heat source case, the ORC described above remains identical with additional system components added including thermal energy storage (TES) system and a solar collector field. The storage type selected is pebble bed (efficiency assumed to be 95%) which can be economical for ORC systems (Hasnain SM, 1998). Modeling details of such a TES system can be found in Kshirsagar et al., 2015. Parabolic trough collector efficiency is modeled as a function of operating HTF temperatures (Kutscher et al., 2012). Solar calculations are performed for Vernal Equinox at the Tropic of Cancer (roughly the mean of extreme Indian latitudes) using the ASHRAE clear sky model. The clearness factor is selected to achieve an annual average DNI of 5.3 kWh/m^2-day. Annual average ambient temperature on such a location is 30 ºC. The thermal energy storage capacity and solar field are sized to ensure steady output of the plant at an ORC capacity factor of 0.5 throughout the year.

3. Methodology

Detailed component level models are developed and integrated in Matlab to simulate the systems described in cases A and B. For the given power capacity, investment cost of these systems is highly dependent on the operating conditions in their power blocks. Optimization proceeds by varying these operating conditions within the 7-dimensional space formed by working fluid type, HTF inlet temperature (heat source temperature), pinch in condenser, regenerator and HEX (boiler), expander inlet pressure and condenser area. The objective function is to minimize the specific cost of the system (C_{sp}) taking into account parasitic losses of working fluid and HTF pumping and fan power in condenser.

$$C_{sp} = \frac{\text{Total investment cost}}{\text{ORC output - parasitic losses}} \quad (1)$$

The algorithm to optimize the above power block is given in Figure 3. The parametric sweep was performed for 3 different power scales, 5, 50 and 500 kWe. Above 500 kWe, the expected technical setup changes (e.g., positive displacement expanders could be replaced by turbines and plunger pumps by centrifugal, etc.), hence this study is confined to small scale ORCs ~500kW_e or below.

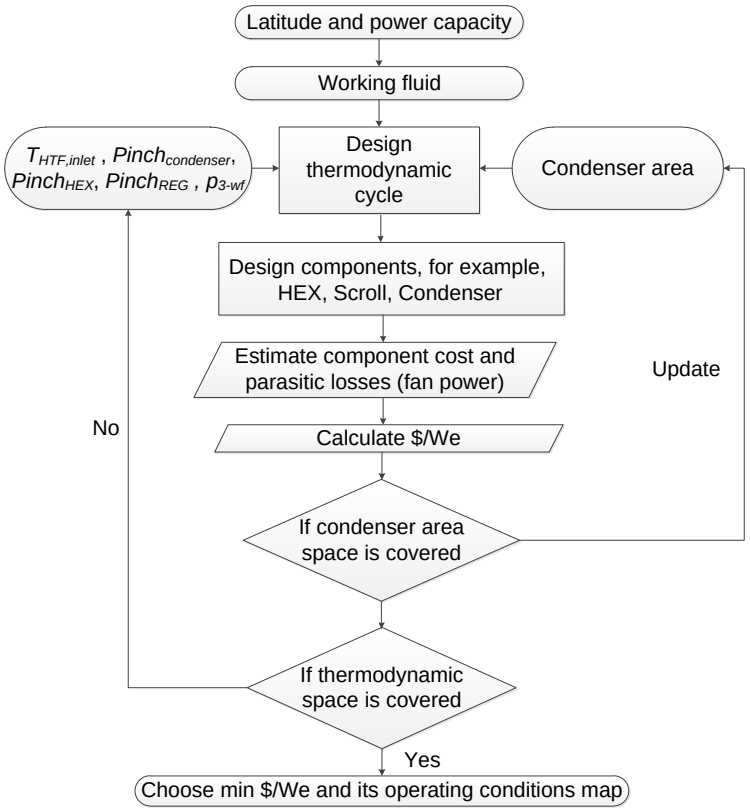

Figure 3. Algorithm to optimize the ORC system on thermo-economic basis

4. RESULTS AND DISCUSSIONS

Optimum C_{sp} values are calculated for 16 zero-ODP and positive condenser pressure (saturation pressure corresponding to 45 ºC) working fluids for HTF supply temperatures between 125 and 275 ºC in steps of 25 ºC for the power capacities of 5, 50 and 500 kWe. To facilitate visualization of the data, only the 8 highest performing fluids are presented here (including ipentane and R245fa, two widely used fluids in ORCs). For some fluids, equations of state in the REFPROP property data base were extrapolated beyond their specified limits to enable a one to one comparison for the given HTF temperature, however, operating temperatures considered are well below the fluid thermal stability temperatures as suggested by Morgan and Munday (1935), Angelino and Invernizzi (2003), Hidaka et al. (2004), Moon et al. (2004) and Ito et al. (2014).

4.1 ORCs connected to geothermal or waste heat sources (Case A)

For a 5 kWe ORC, the optimum C_{sp} values are presented in Figure 4 against HTF_{in} temperature for different working fluids. At any temperature, C_{sp} is found to be a strong function of working fluid type, with a larger variance at lower temperatures; isopentane yields the highest C_{sp} whereas R152a and R161 compete at the low end. The trend for C_{sp} among different fluids is consistent at different temperatures. Certain fluids exhibit a sudden increase in cost with increase in HTF_{in} temperature due to transitioning from a sub to trans-critical cycle or due to excess heat duties of boiler and condenser in cases where a regenerator is not employed. While there is a significant potential for reducing C_{sp} with temperature in the case of isopentane, the same is not true in the case of R152a or R161 where the reduction in cost is just 10 % with increase in HTF temperature from 125 to 275 ºC. Further, Figure 4 illustrates that an increase in efficiency is not always economically advantageous.

The corresponding map of optimum operating conditions is given in Figure 5 wherein the volumetric expansion ratio (v_4/v_3), expander inlet pressure ($p_{3,wf}$), pinch in condenser and HEX, condenser area and regenerator fractional cost are plotted. It is noteworthy that the lowest C_{sp} values are observed at the lowest volumetric expansion ratios in the expander at higher inlet pressures. Volume ratios as high as 20 are observed, requiring a multi stage expansion process or non-conventional scroll

expanders (Orosz et al., 2013). Also, higher pinch temperatures can be tolerated at higher HTF_{in} temperatures. Optimized condensers converge on the smallest size possible in the domain of standard available air-cooled condensers considered. Further, improvement in efficiency via incorporating a regenerator is not economically justified for 5 kWe scale ORCs and hence optimized ORCs do not incorporate the regenerators. The rationale behind the exclusion of a regenerator at 5 kWe is justified by comparing the best cases with and without regenerator for minimum C_{sp} as shown in Figure 6. Also, Decreasing volumetric flow rate at the expander exhaust is found to be a key parameter for lower C_{sp} in cases of high condenser pressure fluids - with the exception of R134a which should have yielded a cost equivalent to that of R152a. In this case the penalty for lack of regenerator is relatively higher than for R152 and R161, where expansion significantly reduces the potential for heat recovery in the regenerator. The above analysis is extended to power scales of 50 and 500 kWe and is represented in Figures 7 to 11. Unexpectedly, the lowest C_{sp} values exhibit a jump at HTF temperature of 175 ºC. At this temperature, power blocks without regenerator demand higher heat duties in HEX and condenser and hence optimum power blocks begin to employ a regenerator, resulting in higher C_{sp}.

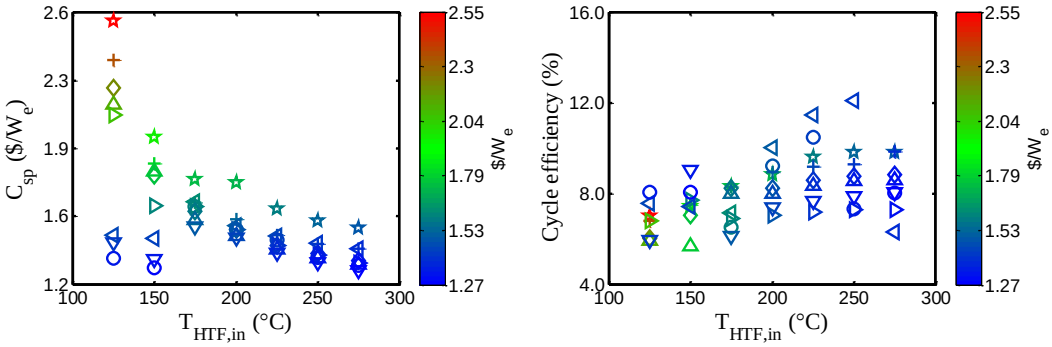

Figure 4. C_{sp} and cycle efficiency for various working fluids against HTF,in temperatures for a 5 kWe ORC. Legend: ☆ ipentane, Δ butane, ▷ isobutane, + R245ca, ◊ R245fa, ◁ R134a, ○ R161, ▽ R152a.

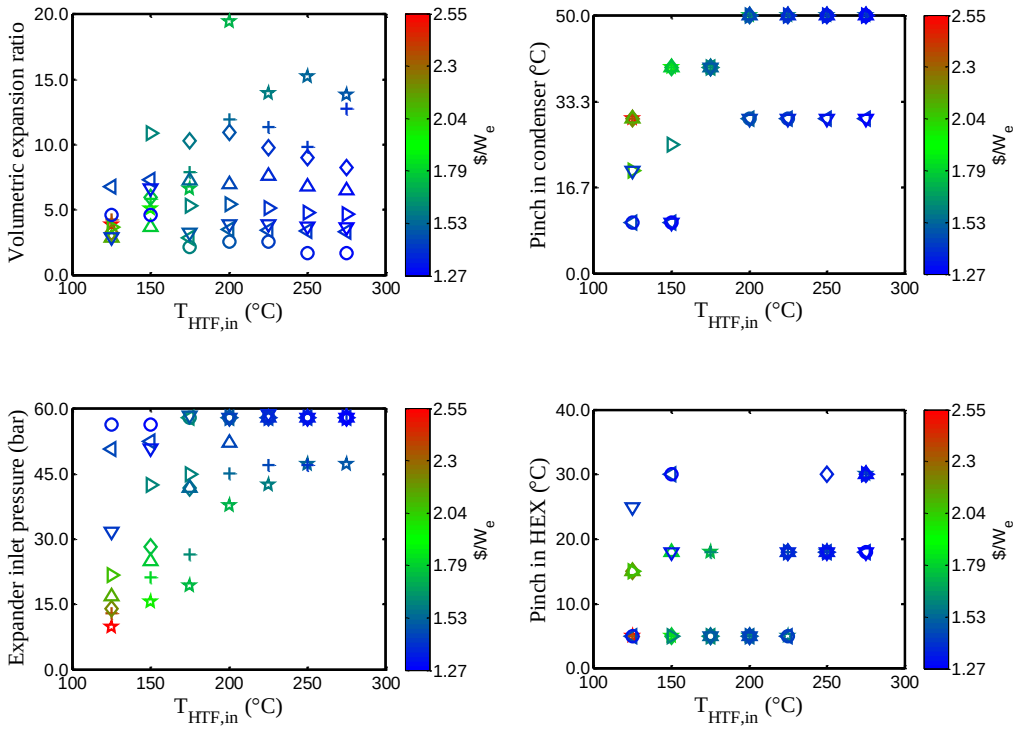

Figure 5. Corresponding map of optimum operating parameters for various working fluids against HTF,in temperatures for a 5 kWe ORC. Legend: ☆ ipentane, Δ butane, ▷ isobutane, + R245ca, ◊ R245fa, ◁ R134a, ○ R161, ▽ R152a.

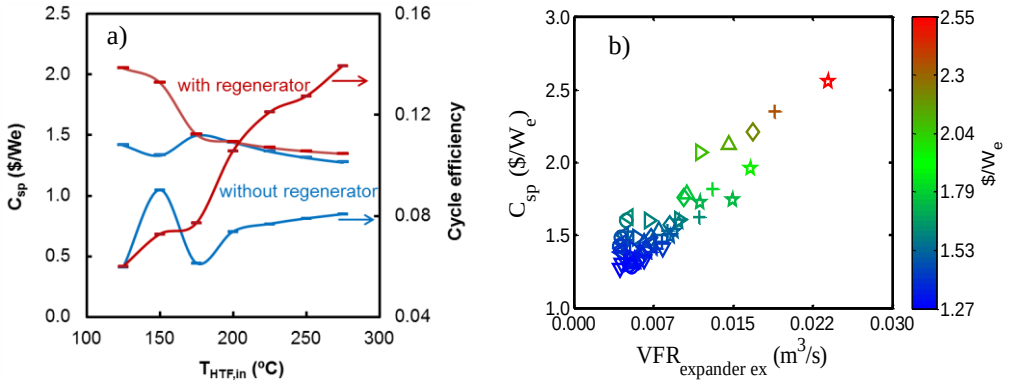

Figure 6. a) Comparison of the best cases with and without regenerator for minimum C_{sp} for a 5 kWe R152ORC. b) C_{sp} against the volumetric flow rate at the expander exhaust. Legend: ☆ isopentane, Δ butane, ▷ isobutane, + R245ca, ◊ R245fa, ◁ R134a, ○ R161, ▽ R152a.

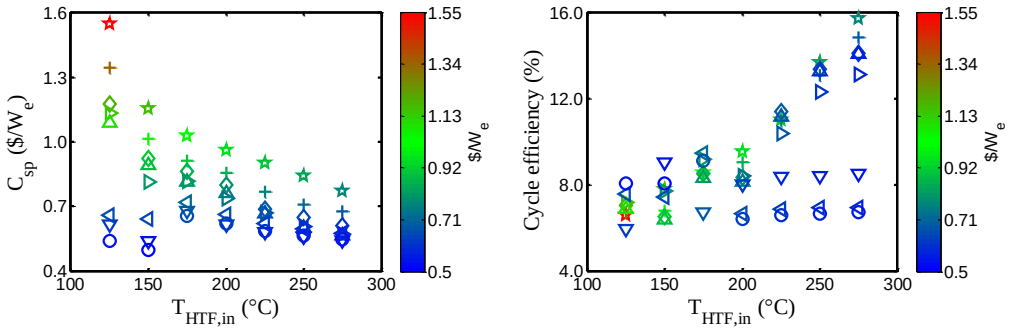

Figure 7. C_{sp} and cycle efficiency for various working fluids against HTF,in temperatures for a 50 kWe ORC. Legend: ☆ ipentane, Δ butane, ▷ isobutane, + R245ca, ◊ R245fa, ◁ R134a, ○ R161, ▽ R152a.

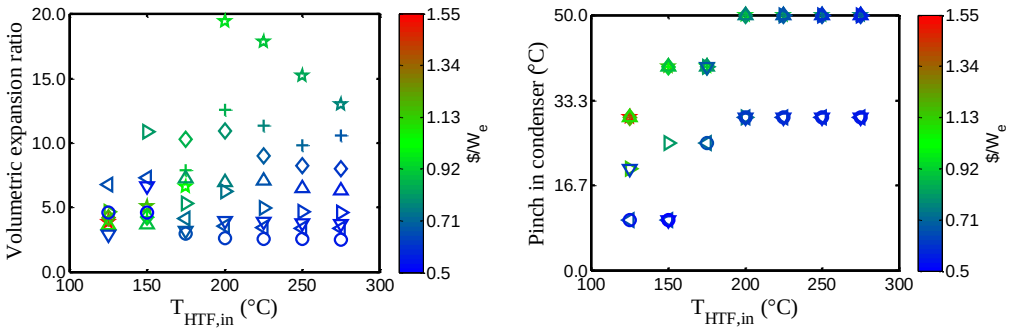

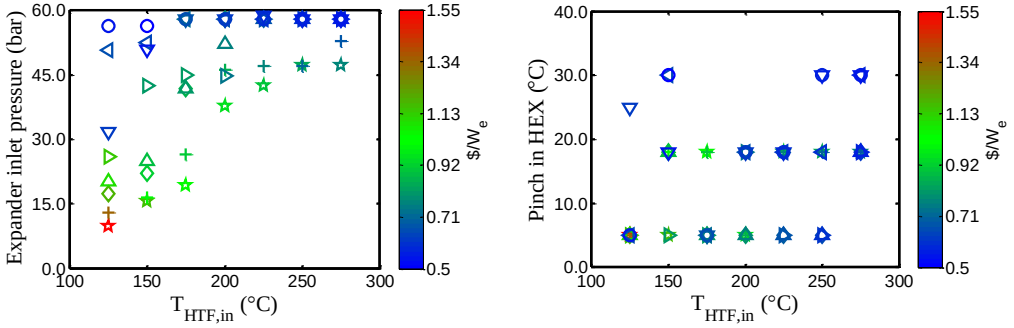

Figure 8. Corresponding map of optimum operating parameters for various working fluids against HTF,in temperatures for a 50 kWe ORC. Legend: ☆ ipentane, ∆ butane, ▷ isobutane, + R245ca, ◊ R245fa, ◁ R134a, ○ R161, ▽ R152a.

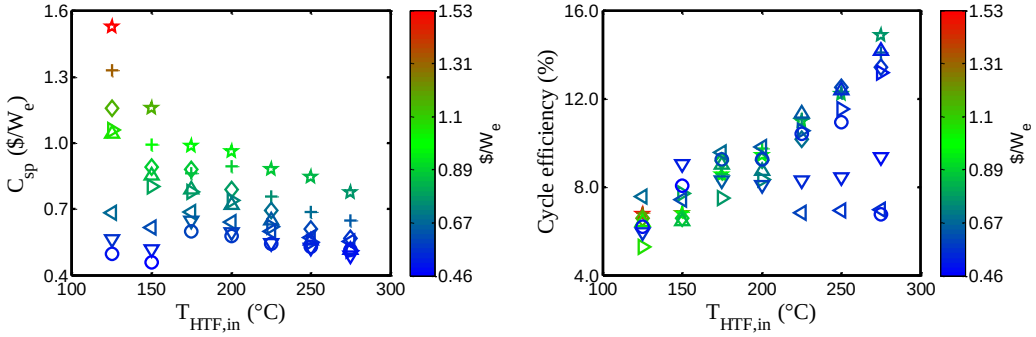

Figure 9. C_{sp} and cycle efficiency for various working fluids against HTF,in temperatures for a 500 kWe ORC. Legend: ☆ ipentane, ∆ butane, ▷ isobutane, + R245ca, ◊ R245fa, ◁ R134a, ○ R161, ▽ R152a.

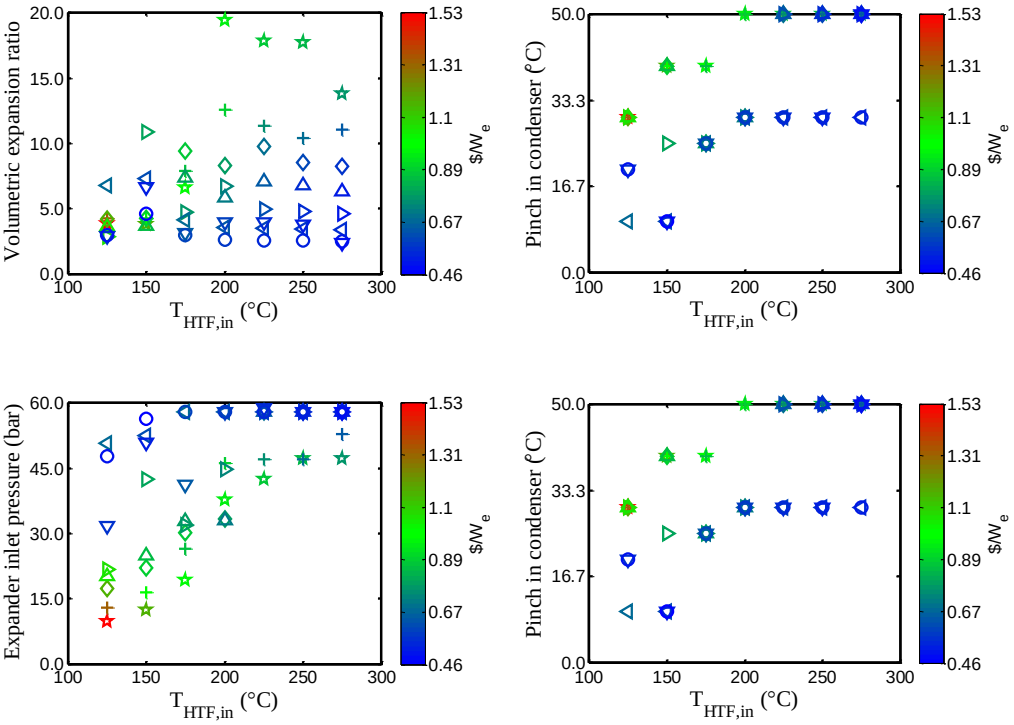

Figure 10. Corresponding map of optimum operating parameters for various working fluids against HTF,in temperatures for a 500 kWe ORC. Legend: ☆ ipentane, Δ butane, ▷ isobutane, + R245ca, ◊ R245fa, ◁ R134a, ○ R161, ▽ R152a.

A cost break-down of the lowest C_{sp} ORC configurations is presented in Figure 11 for the power scales of 5, 50 and 500 kWe. At 5 kWe, instrumentation, DAQ system and controls represents a proportionally high fraction of total system costs, followed by ACC, scroll expander, pumps and HEX. The trend is reversed as the power scale goes up. While the absolute cost of instrumentation remains almost constant, the cost of volumetric machinery (pumps and scroll expander) scales linearly.

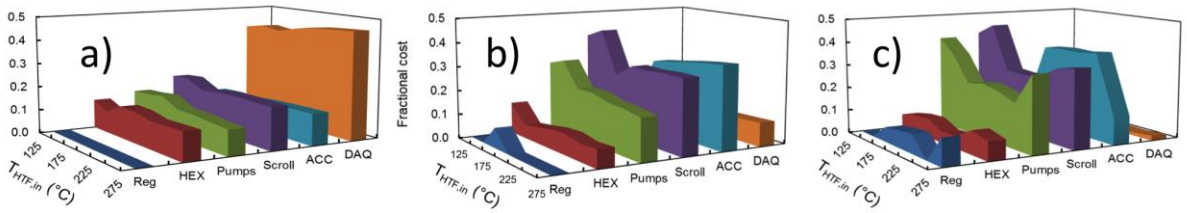

Figure 11. Cost break up for ORCs with lowest specific costs at various HTF operating temperatures. a) 5 kWe, b) 50 kWe and c) 500 kWe. Pump costs are inclusive of working fluid, HTF pumps and their VFD drives.

4.2 ORCs connected to solar heat source (Case B)

The initial investment cost for a solar-ORC per unit power produced is presented in Figure 12 for the different working fluids against HTF_{in} temperature. At lower HTF operating temperatures, these costs are an order of magnitude higher than in ORCs with "free" thermal sources (Case A), but decrease by a factor of 4 across the range of HTF_{in} temperatures, indicating the advantage of moving to higher operating temperatures. The trend among the working fluids is reversed with isopentane offering the lowest C_{sp} values and R161 or R152a the highest. Further, at higher HTF temperatures, there exist two distinct clusters of working fluids, at higher and lower costs levels. This trend can be mapped on the efficiency plot in Figure 12, emphasizing the fact that lower C_{sp} values are the direct result of higher cycle efficiencies, which in turn minimize the solar field area required and its associated cost. The corresponding map of optimum operating parameters is given in Figure 13. In solar-ORCs, this parameter space adjusts itself to maximize the cycle efficiency and hence pinch temperatures in condenser, regenerator and HEX tend to be minimized and ORCs tend to be regenerative. Similar exercises have been repeated for different power scales and are presented in Figures 14-17.

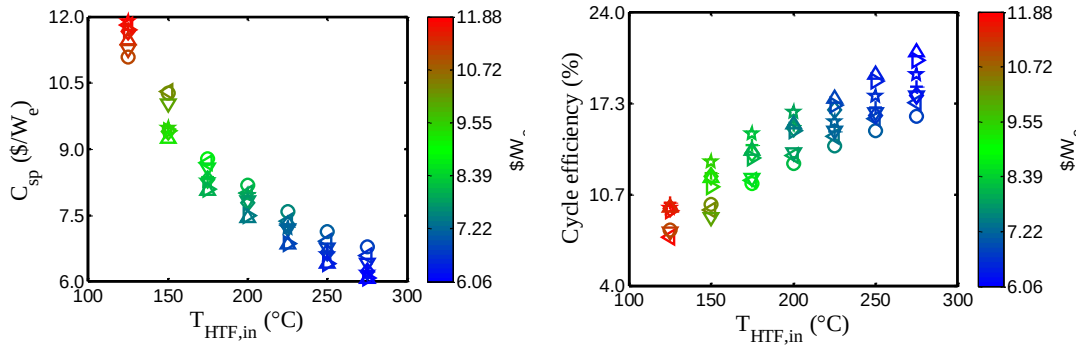

Figure 12. C_{sp} and cycle efficiency for various working fluids against HTF,in temperatures for a 5 kWe solar-ORC. Legend: ☆ ipentane, Δ butane, ▷ isobutane, + R245ca, ◊ R245fa, ◁ R134a, ○ R161, ▽ R152a.

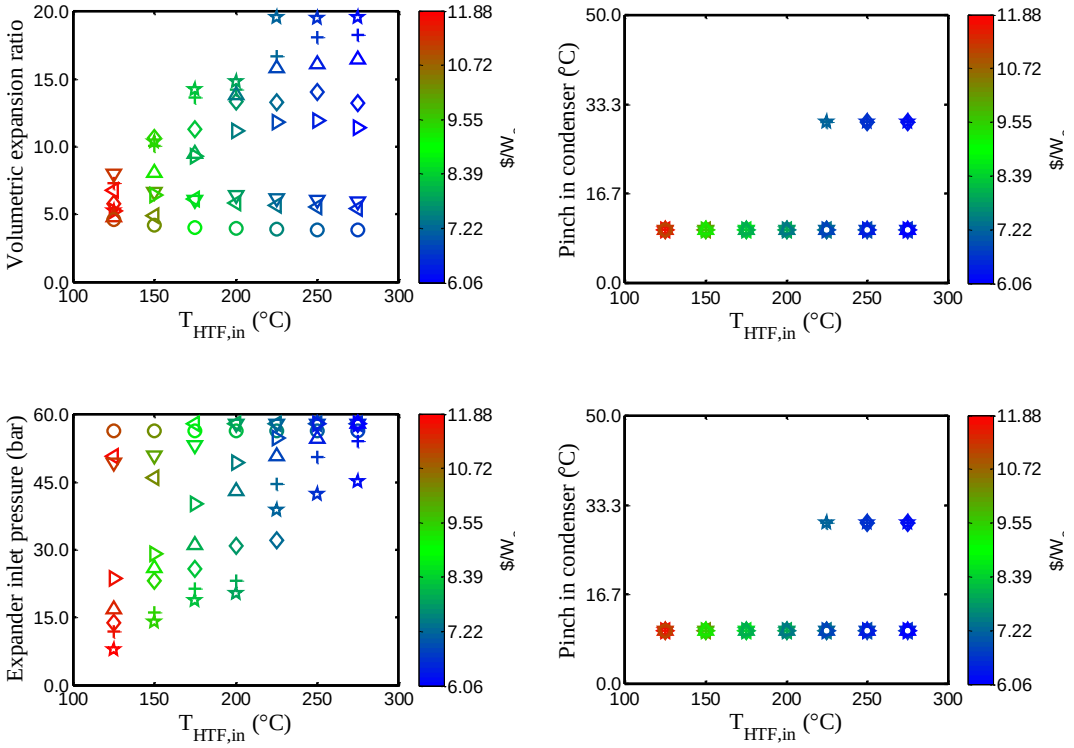

Figure 13. Corresponding map of optimum operating parameters for various working fluids against HTF,in temperatures for a 5 kWe solar-ORC. Legend: ☆ ipentane, Δ butane, ▷ isobutane, + R245ca, ◊ R245fa, ◁ R134a, ○ R161, ▽ R152a.

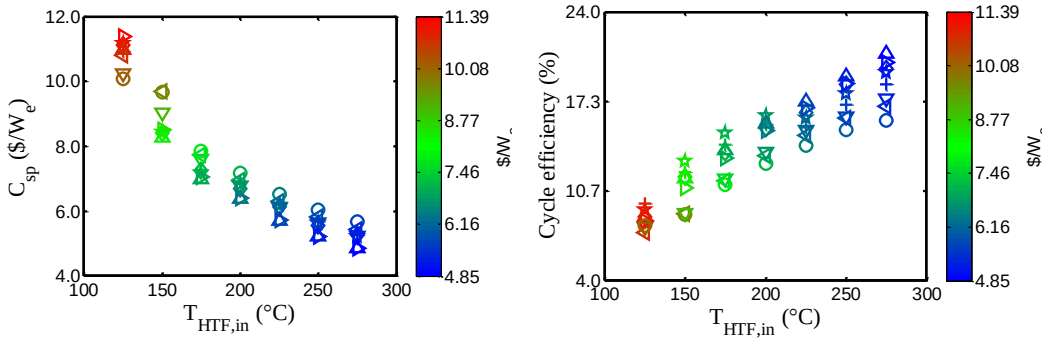

Figure 14. C_{sp} and cycle efficiency for various working fluids against HTF,in temperatures for a 50 kWe solar-ORC. Legend: ☆ ipentane, Δ butane, ▷ isobutane, + R245ca, ◊ R245fa, ◁ R134a, ○ R161, ▽ R152a.

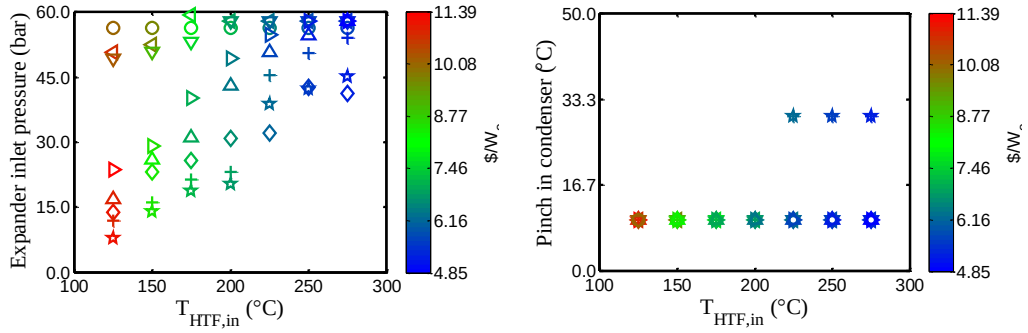

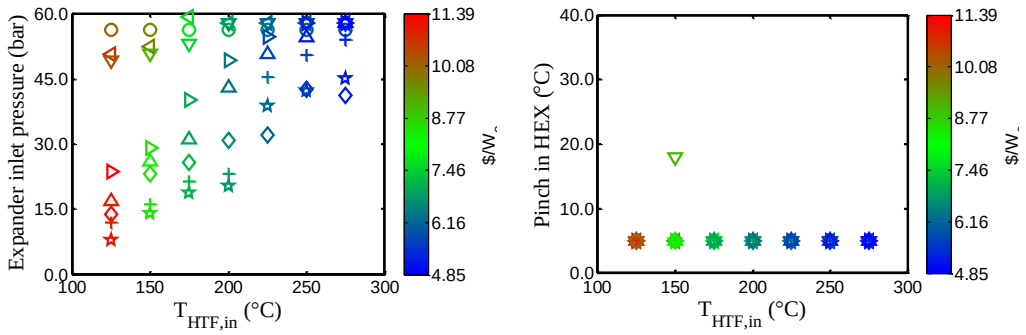

Figure 15. Corresponding map of optimum operating parameters for various working fluids against HTF,in temperatures for a 50 kWe solar-ORC. Legend: ☆ ipentane, Δ butane, ▷ isobutane, + R245ca, ◊ R245fa, ◁ R134a, ○ R161, ▽ R152a.

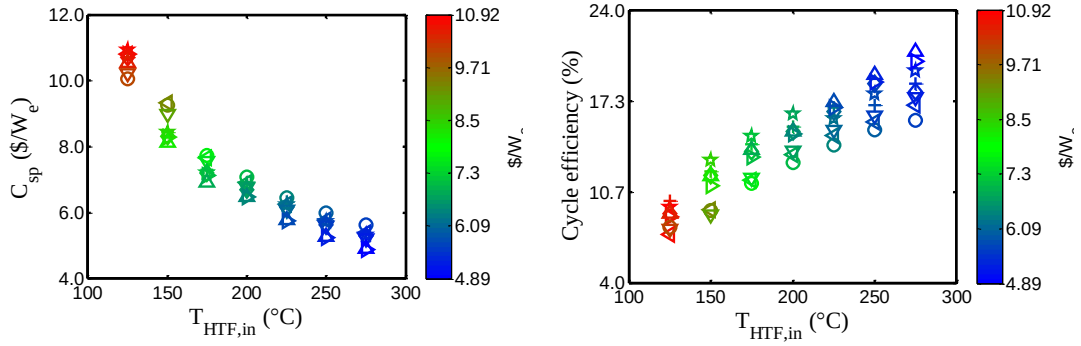

Figure 16. C_{sp} and cycle efficiency for various working fluids against HTF,in temperatures for a 500 kWe solar-ORC. Legend: ☆ ipentane, Δ butane, ▷ isobutane, + R245ca, ◊ R245fa, ◁ R134a, ○ R161, ▽ R152a.

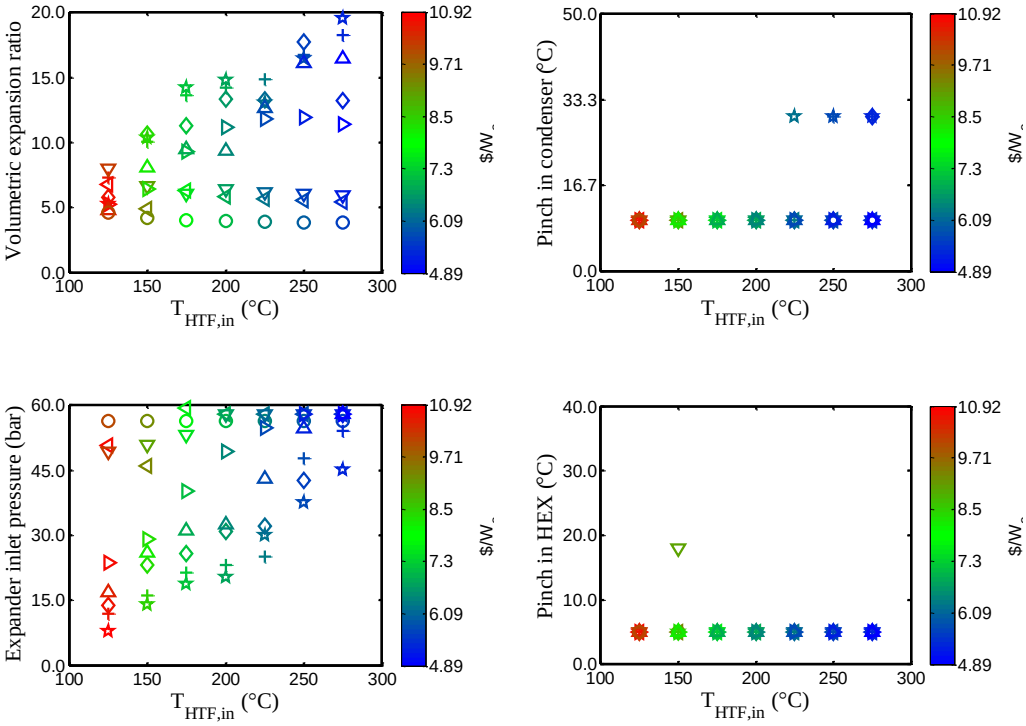

Figure 17. Corresponding map of optimum operating parameters for various working fluids against HTF,in temperatures for a 500 kWe solar-ORC. Legend: ☆ ipentane, Δ butane, ▷ isobutane, + R245ca, ◊ R245fa, ◁ R134a, ○ R161, ▽ R152a.

Cost break-down for solar-ORCs is plotted in Figure 18 which indicates the solar field cost to be highest followed by power block and then storage system. Potential for further decrease in specific cost lies in the realization of higher temperature ORCs.

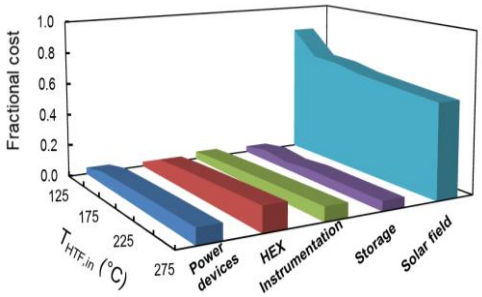

Figure 18. Cost break up of solar-ORCs with lowest specific costs at various HTF operating temperatures. 5 kWe is shown and 50 kWe and 500 kWe are omitted due to their close visual similarity. While power devices include pumps and expander, heat exchangers include regenerator, HEX and condenser.

Conclusions

The variable space formed by HTF supply temperature, pinch in condenser, regenerator and boiler, expander inlet pressure, condenser area and working fluid affects the ORC investment cost in a significant way. A tool developed to analyze the design space is applied for two major applications of ORCs, namely geothermal/waste heat and solar. The conclusions drawn from these two studies are well distinguished and summarized as follows:

ORC coupled to geothermal/waste heat source

i. At any given temperature, R152a and R161 are found to yield the lowest cost. This cost pattern is attributed to their higher condenser pressures which imply lower volumetric flow rates at the expander exit (state of maximum volumetric flow rate) resulting in compact fluid machinery.

ii. Some smaller ORCs may optimize their specific costs without incorporating a regenerator

iii. Instrumentation costs are proportionally higher for smaller ORCs

iv. Increase in HTF supply temperature does not yield a significant decrease in the lowest specific cost indicating diminishing returns with increased operating temperature.

ORC coupled to solar heat source

i. Isopentane emerges as the best working fluid in solar ORCs at low HTF temperatures. However, at elevated temperatures, isopentane, R245fa and R245ca costs converge.

ii. The regenerator cost is justified even at lower temperatures and lower power scales owing to higher cycle efficiencies and lower solar field costs.

iii. The lowest cost of power generation at 5, 50 and 500 kWe are observed to be 5.9, 4.72 and 4.71 $/We, respectively indicating asymptotic behavior of cost beyond 50 kWe.

iv. Storage cost associated with a TES system designed for damping the solar insolation fluctuations on the power block side are found to be ~ 75 % of the power block. However, solar field cost remains a major contributing factor towards the total solar-ORC cost motivating to search for high temperature and hence more efficient ORCs requiring lower lower solar field area.

This work can contribute towards best practices that improve cost effectiveness of distributed ORCs. Future work involves the evaluation of the levelized cost of energy and appropriate business strategies for target ORC applications.

REFERENCES

Angelino, G., Invernizzi, C. M., 2003, Experimental investigation on the thermal stability of some new zero ODP refrigerants, *Int. J. of Refrigeration*, 26, 1, 51-58

Fiaschi, D., Manfrida, G., Maraschiello, F., 2012, Thermo-fluid dynamics preliminary design of turbo-expanders for ORC cycles, *Applied Energy*, 97, 601–608.

Garg, P., Kumar, P., Srinivasan, K., Dutta, P., 2013, Evaluation of isopentane, R-245fa and their mixtures as working fluids for organic Rankine cycles, *Applied Thermal Engineering*, 51, 292-300

Hasnain, SM. Review on sustainable thermal energy storage technologies. Part1. Heat storage materials and techniques, *Energy Convers Manage*, J1998, 39, 11, 1127–38

Hidaka, Y., Oki, T., Kawano, H., 2004, Thermal Decomposition of Propane in Shock Waves, *Int J. of Chemical Kinetics*, 21 , 8, 1

Hung, T.C., Wang, S.K., Kuo, C.H., Pei, B.S., Tsai, K.F., 2010, A study of organic working fluids on system efficiency of an ORC using low-grade energy sources, *Energy*, 35, 3, 1403–1411

Ito, M., Dang, C., Hihara, E., 2014, Thermal Decomposition of Lower-GWP Refrigerants, 15th *Int. Refrigeration & Air conditioning Conference*, 2591,1-10

Kshirsagar, A., Garg, P., Kumar, P., Orosz, M.S., 2015, Identification of ORC parameters for optimization of thermal storage medium cost in solar ORC, accepted in ASME ORC 2015.

Kutscher, C., Burkholder, F., Stynes, K., 2012, Generation of a Parabolic Trough Collector Efficiency Curve from Separate Measurements of Outdoor Optical Efficiency and Indoor Receiver Heat Loss, *J. of Solar Energy Engineering*, 134 / 011012-1, 1-6

Lecompte, S., Huisseune, H., Broek, M.V.D., Schampheleire, S.D., Paepe, M.D., 2013, Part load based thermo-economic optimization of the Organic Rankine Cycle (ORC) applied to a combined heat and power (CHP) system, *Applied Energy*, 111, 871–881

Lemort ,V., Qoulin ,S., Cuevas ,C., Lebrun ,J., 2009, Testing and modelling a scroll expander integrated into an Organic Rankine Cycle, *Applied Thermal Engineering*, 29, 14-15, 3094–3102

Maizza, V., Maizza, A., 2001, Unconventional working fluids in organic Rankine-cycles for waste energy recovery systems, *Applied Thermal Engineering*, 21, 3, 381–390

Martin, H., 1996, A theoretical approach to predict the performance of chevron-type plate heat exchangers, *Chemical Engineering and Processing: Process Intensification* 35 (4), 301-310

Moon, D.J., Chung ,M.J., Kwon ,Y.S., Ahn ,B.S., 2004**,** Thermally decomposing difluorochloromethane to tetrafluoroethylene; dimerization in fluidized bed reactor, *US6710215B2*

Morgan, J.J., Munday, J.C., 1935, Thermal Decomposition of n-Pentane, *Industrial and Engineering Chemistry*, 27, 9, 1081-1086

Orosz, M.S., Mueller, A.V., Dechesne, B.J., Hemond H.F., 2013, Geometric Design of Scroll Expanders Optimized for Small Organic Rankine Cycles, *J. Eng. Gas Turbines Power*, 135(4), 042303

Qoulin, S., Declaye, S., Tchanche, B.F. , Lemort, V., Thermo-economic optimization of waste heat recovery Organic Rankine Cycles, 2011, *Applied Thermal Engineering*, 31, 14-15, 2885–2893

Tempesti, D., Fiaschi, D., 2013, Thermo-economic assessment of a micro CHP system fuelled by geothermal and solar energy, *Energy*, 58, 45–51

Velez, F., Segovia, J.J., Martin ,M.C., Antolin ,G., Chejne ,F., Quijano ,A., 2012, A technical, economical and market review of organic Rankine cycles for the conversion of low-grade heat for power generation, *Renewable and Sustainable Energy Reviews*, 16, 6, 4175–4189

Wang, E.H., Zhang, H.G., Fan, B.Y., Ouyang, M.G., Zhao, Y., Mu, Q.H., 2011, Study of working fluid selection of organic Rankine cycle (ORC) for engine waste heat recovery, *Energy*, 36, 5, 3406–3418

Wei, D., Lu, X., Lu, Z., Gu, J., 2007, Performance analysis and optimization of organic Rankine cycle (ORC) for waste heat recovery, *Energy Conversion and Management*, 48, 4, 1113–1119

Wright, M.F., 2000, Plate-fin-and-tube condenser performance and design for refrigerant R-410a air-conditioner, *Submitted as Master's Thesis at Georgia Institute of Technology.*

Würfel, R., Ostrowski, N., 2004, Experimental investigations of heat transfer and pressure drop during the condensation process within plate heat exchangers of the herringbone-type, *International Journal of Thermal Sciences*, 43, 59–68

Pioro, I.L., Khartabil1, H.F., Duffey, R.B., 2004, Heat transfer to supercritical fluids flowing in channels—empirical correlations (survey), *Nuclear Engineering and Design*, 230, 69–91

ACKNOWLEDGEMENT

This research is based upon work supported by the Solar Energy Research Institute for India and the U.S. (SERIIUS) funded jointly by the U.S. Department of Energy subcontract DE AC36-08G028308 (Office of Science, Office of Basic Energy Sciences, and Energy Efficiency and Renewable Energy, Solar Energy Technology Program, with support from the Office of International Affairs) and the Government of India subcontract IUSSTF/JCERDC-SERIIUS/2012 dated 22nd Nov. 2012.

APPENDIX A

Cost functions for various components in US Dollars are as follows:

$$cost_{PHE} = 492.76 + 609.6A_{heat-transfer} \quad \text{(A.1)}$$

$$cost_{ACC} = NPU(1000A_{fan} + 173.3) \quad \text{(A.2)}$$

$$cost_{scroll} = (266.2 + 170976VFR_{outlet})\left(0.6858 + 0.2732\ln\left(\frac{VFR_{outlet}}{VFR_{inlet}}\right)\right) \quad \text{(A.3)}$$

$$cost_{tank} = 130V + 1140 \quad \text{(A.4)}$$

$$cost_{pump} = 19.7VFR_{inlet} \quad \text{(A.5)}$$

$$cost_{VFD} = 93.6\dot{W} + 110.1 \quad \text{(A.6)}$$

$$cost_{alternator} = 56.5\dot{W} + 8.9 \quad \text{(A.7)}$$

$$cost_{solar-field-per-sq.meter} = 245 \quad \text{(A.8)}$$

Cost per kg of the working fluids and HTFs considered is as follows:

$$cost_{ipentane} = 2.85 \quad \text{(A.9)}$$

$$cost_{R152a} = 3.51 \quad \text{(A.10)}$$

$$cost_{R134a} = 5.85 \quad \text{(A.11)}$$

$$cost_{isobutan} = 4.68 \quad \text{(A.12)}$$

$$cost_{R245ca} = 13.6 \quad \text{(A.13)}$$

$$cost_{butane} = 3.4 \quad \text{(A.14)}$$

$$cost_{R245fa} = 12.4 \quad \text{(A.15)}$$

$$cost_{R161} = 12.36 \quad \text{(A.16)}$$

$$cost_{EG,per,kg} = 1.6 \quad \text{(A.17)}$$

$$cost_{\text{Therminol-VP1},per,kg} = 5.8 \quad \text{(A.18)}$$

Cost of instrumentation is as follows:

$$cost_{pressure-sensor} = 200 \quad \text{(A.19)}$$

$$cost_{temperature-gauge} = 50 \quad \text{(A.20)}$$

$$cost_{current-transducer} = 100 \quad \text{(A.21)}$$

$$cost_{relay} = 65 \quad \text{(A.22)}$$

$$cost_{data-aquisition} = 300 \quad \text{(A.23)}$$

$$cost_{processor} = 250 \quad \text{(A.24)}$$

$$cost_{user-interface} = 65 \quad \text{(A.25)}$$

$$cost_{network-cabel} = 300 \quad \text{(A.26)}$$

Number of instrument components considered as follows: